Direct Observation of "Pure MEL Type" Zeolite

Osamu Terasaki,*,† Tetsu Ohsuna,‡ Hiroshi Sakuma,† Denjiro Watanabe,‡ Yumi Nakagawa,§ and Ronald C. Medrud§

Department of Physics, Faculty of Science, Tohoku University, Sendai 980-77, Japan; College of Science and Engineering, Iwaki Meisei University, Iwaki, Fukushima 970, Japan; and Chevron Research and Technology Company, 100 Chevron Way, Richmond, California

Received August 16, 1995. Revised Manuscript Received October 23, 1995⊗

We have obtained the direct evidence by high-resolution electron microscopy (HREM) that a pure MEL type zeolite has been successfully synthesized in an all-silica form using a novel organocationic templating agent. It has been also confirmed from a synchrotron X-ray powder diffraction pattern obtained at room temperature that the crystal structure of this all-silica zeolite is of the MEL-type by use of the Rietveld method.

Introduction

More than 15 years has passed since the first report of ZSM-11(MEL-type) by Kokotailo et al. The structure originally proposed was based on X-ray powder diffraction studies and model building.[1] The authors described the framework structures of MFI(ZSM-5) and MEL as the two end members of the same family with the same structure (pentasil) unit.[2] MEL has the highest symmetry of all the members, belonging to the space group $I\bar{4}m2$, and consequently its powder X-ray diffraction pattern should have the fewest number of reflections. ZSM-5 has been widely studied due to its attractive catalytic properties. Although MEL shares many similar structural features with MFI, fewer studies on MEL have been reported, perhaps due to difficulties in synthesizing this material. Recently, using a combination of high-resolution solid-state NMR and synchrotron X-ray powder diffraction data, it has been claimed that a postsynthetically dealuminated high-silica ZSM-11 sample contained very few of the stacking faults proposed by Perego et al.[3−7] The authors noted that diffuse scattering was observed at around 15, 21, and 25° and speculated this might be due to amorphous material,[5,6] although this was not observed in the fist report.[4] They also stressed that the peak-to-background intensity ratio for the strong (101) reflection is about 300:1 because of the well-crystallized sample.[4] This ratio, however, can be achieved using conventional X-ray equipment if the sample crystallinity is good. To our knowledge, there has yet to be reported any direct experimental evidence for the existence of a pure MEL-type zeolite.[8,9] Using electron microscopy (EM), we have examined many specimens from different sources which were claimed to be ZSM-11, but all appear to be MFI-type material with faults. This is consistent with the well-known fact that it is difficult to obtain MEL crystals which are free of intergrowths of the MFI-type. In contrast, a large and high-quality single crystal of an MFI-type has been synthesized, and hence several precise structure analyses have been reported, e.g., it has been reported that calcined ZSM-5 has a low-temperature form of $P2_1/n$ which transforms to a high-temperature form of $Pnma$ at ca. 340 K.[10,11] Similarly, Fyfe et al. reported that the dealuminated high-silica ZSM-11 exhibited a phase transition from a room-temperature phase (which they speculate to be $I\bar{4}$) to a high-temperature phase ($I\bar{4}m2$) at ca. 320 K.[6,7]

In principle, it is not difficult to differentiate MFI- and MEL-type zeolites, especially if pure-phase MEL is available for comparison. X-ray diffraction techniques can discern the difference based on their different symmetries, i.e., $Pnma$ and $I\bar{4}m2$, and their unit-cell parameters. For example, based on the extinction rule, $hk0$ reflections with both h and k = odd (i.e., 110 reflection at 6.2° and 330 at 18.7° for Cu Kα radiation) are allowed for MEL but not for MFI. Also, the hkl and khl reflections are doublets for MFI whereas they appear as a singlet for MEL-type materials. A diffuclty often arises as the ratio of lattice constants a/b approaches 1.0. However, this is usually due to the fact that specimens are *not* pure MEL-type and that they contain many faults.

By using transmission electron microscopy (TEM), it is very simple (even from very small crystallites) to check whether the specimen is pure phase or not, to characterize structure defects, and to distinguish between MFI- and MEL-type materials.[8,9] In addition, if the zeolite is highly crystalline, its crystal morphology, which is observable using scanning electron microscopy

† Tohuku University.
‡ Iwaki Meisei University.
§ Chevron Research and Technology Co.
⊗ Abstract published in *Advance ACS Abstracts*, December 1, 1995.

(1) Kokotailo, G. T.; Chu, P.; Lawton, S. L.; Meier, W. M. *Nature* **1978**, *275*, 119.
(2) Kokotailo, G. T.; Meier, W. M. Pentasil family of high silica crystalline materials. *The properties and applications of zeolites*; Townsend, R. P., Eds.; The Chemical Society: London, 1980; pp 133−139.
(3) Perego, G.; Cesari, M.; Allegra, G. *J. Appl. Crystallogr.* **1984**, *17*, 403.
(4) Toby, B. H.; Eddy, M. M.; Fyfe, C. A.; Kokotailo, G. T.; Strobl, H.; Cox, D. E. *J. Mater. Res.* **1988**, *3*, 563.
(5) Fyfe, C. A.; Gies, H.; Kokotailo, G. T.; Pasztor, C.; Strobl, H.; Cox, D. E. *J. Am. Chem. Soc.* **1989**, *111*, 2470.
(6) Gies, H.; Marler, B.; Fyfe, C.; Kokotailo, G.; Feng, Y.; Cox, D. E. *J. Phys. Chem. Solids* **1991**, *52*, 1235.
(7) Fyfe, C. A.; Feng, Y.; Grondey, H.; Kokotailo, G. T.; Mar, A. *J. Phys. Chem.* **1991**, *95*, 3747.
(8) Millward, G. R.; Ramdas, S.; Thomas, J. M.; Barlow, M. T. *J. Chem. Soc., Faraday Trans. 2* **1983**, *79*, 1075.
(9) Terasaki, O.; Thomas, J. M.; Millward, G. R.; Watanabe, D. *Chem. Mater.* **1989**, *1*, 158.
(10) van Koningsveld, H.; van Bekkum, H.; Jansen, J. C. *Acta Crystallogr.* **1987**, *B43*, 127.
(11) van Koningsveld, H.; Jansen, J. C.; van Bekkum, H. *Zeolites* **1990**, *10*, 235.

0897-4756/96/2808-0463$12.00/0

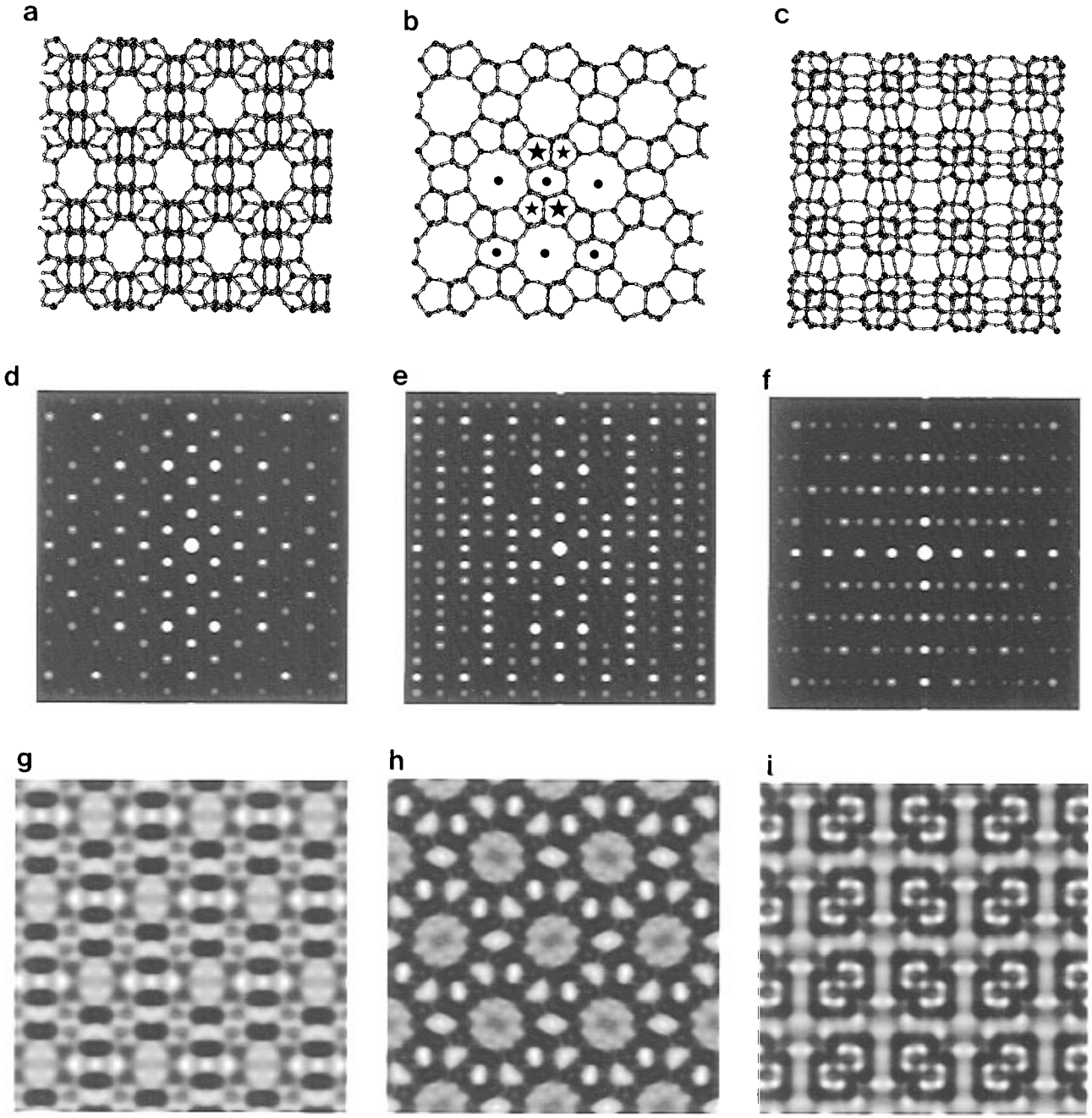

Figure 1. Projections of the framework structure of MFI-type along [100] (a), [010] (b) and [001] (c). Simulated ED patterns (d−f) and HREM images (g−i) of MFI-type along [100], [010], and [001], respectively.

(SEM), provides information on the point symmetry of the crystal, which is very useful for the space group determination. Furthermore we can observe surface steps which are induced by defects through high-resolution SEM images.[12] EM is therefore the most powerful technique for this type of investigation.

Characteristics of MFI and MEL-type crystals are summarized below:

MFI type: A single crystal of MFI shows a nice crystal morphology which is compatible with the point group of *mmm* (for the sapce group *Pnma*) as shown in Figure 2a. Figure 1a−c shows projections of the framework structure of MFI along [100], [010], and [001], respectively. One can clearly observe the 2-fold rotational axes at the points marked by dots in the projection along the [010] in Figure 1b, which correspond to inversion centers for three dimensions and also the mirror plane parallel to (010) in the [001] projection (Figure 1c). Figure 1d−f shows simulated electron diffraction (ED) patterns (for specimen thickness of 100 Å) corresponding to Figure 1a−c, respectively, by taking dynamical scattering of electrons into account. Simulated high-resolution electron microscope (HREM) images at the same crystal thickness, for 400 kV EM at Scherzer focus, are shown in Figure 1g−i.

MEL type: The crystal morphology of MEL must be compatible with $\bar{4}m2$ as illustrated in Figure 2 for the space group of $I\bar{4}m2(b)$ and $\bar{4}$ for the $I\bar{4}(c)$. Figure 3a,b shows the framework structure of MEL along [100] and [001]. Since MEL belongs to the tetragonal system, the [100] and [010] directions are equivalent, and there is a 4-fold axis along the [001] direction. Figures 3c−d and 3e−f show simulated ED patterns and HREM images for 400 kV EM (specimen thickness 100 Å) at

(12) Terasaki, O.; Ohsuna, T. *Catal. Today* **1995**, *99*, 201.

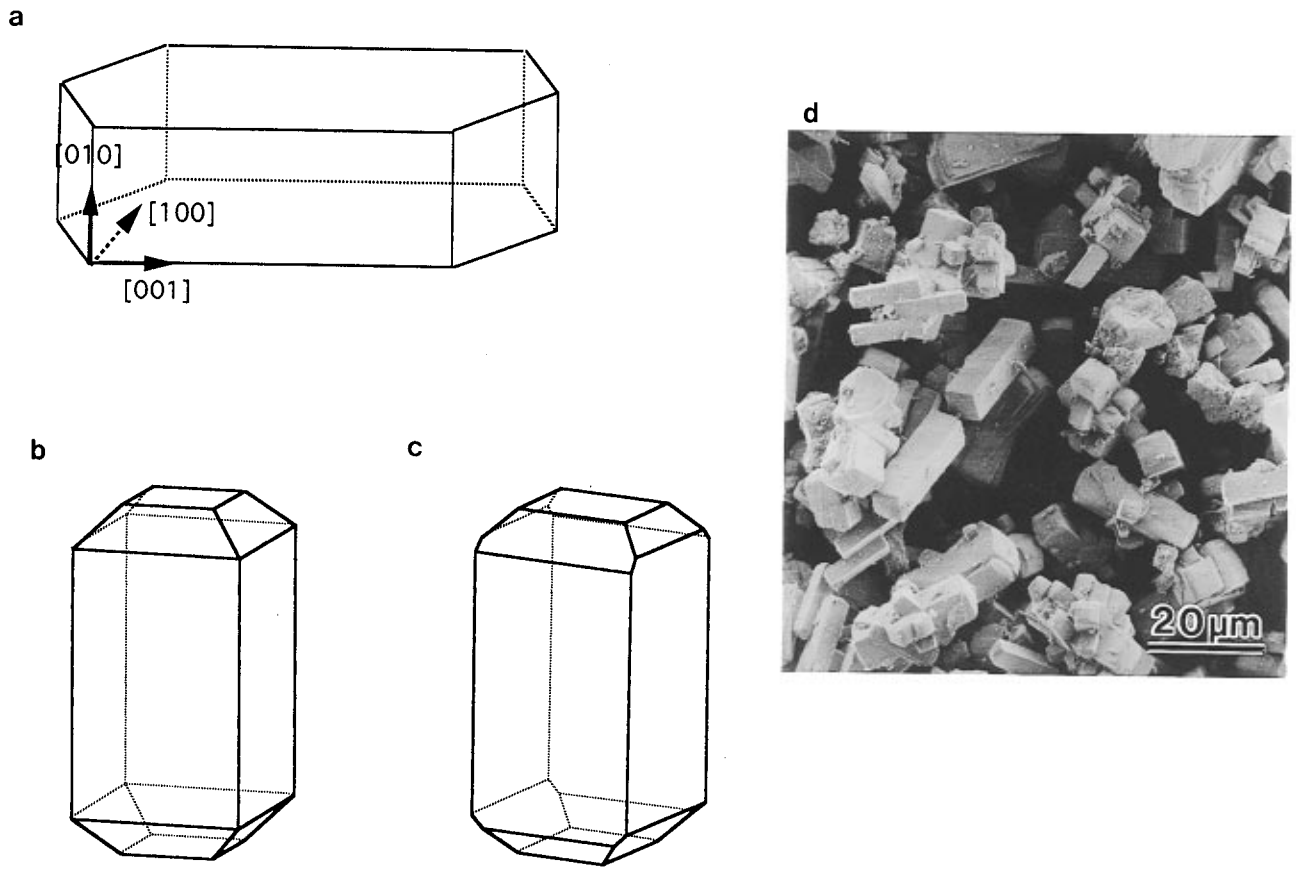

Figure 2. Schematic drawings of external morphology of MFI-type (ZSM-5) (a), and MEL-type (ZSM-11) with a space group of $I\bar{4}m2$ (b) and $I\bar{4}$ (c). Observed SEM image of pure silica MEL type after calcination (d).

Scherzer focus, along the [100] and [001] directions, respectively.

How to differentiate the two types: Comparing the two sets of HREM images and ED patterns for MFI and MEL, it is very clear that the [001] incidence is the best orientation to observe the difference between the two types. Since the symmetry of the projection along the [001] is *p*2*gm* for MFI and *p*4*mm* for MEL, either the ED pattern or the HREM image alone is sufficient to differentiate between the two. In the other two principal directions [100] and [010], we must observe both an ED pattern and an HREM image *as a set* in order to demonstrate that the crystal is the MEL type. The ED pattern in Figure 1d is very similar to that in Figure 3c, but the corresponding HREM images are quite different as shown in Figures 1g and 3e. To observe the small difference in HREM images between Figures 1h and 3e, it is necessary to distinguish between the two different types of 5-rings, which are indicated by two different stars in Figures 1b and 3a, as different contrast or as different size.[9]

If the ED pattern of Figure 1e is observed, the conclusion is that the crystal is of the MFI type. If the crystal is an intergrowth of MFI and MEL types, one can observe diffuse streaks and must be very careful to analyze the streaks in the ED pattern which are produced by many different kinds of defects and manners of intergrowth. This problem has been discussed in detail by Millward et al.[8] In contrast, using our HREM images, we can specify their local structure clearly.[9]

In this report, we will show for the first time, directly and with sufficient experimental evidence, that a pure MEL type zeolite has been synthesized.

Experimental Section

Specimen preparation: All-silica ZSM-11 can be directly synthesized using various sources of silica in the presence of the organocationic templating agent, *N*,*N*-diethyl-3,5-dimethylpiperidinium hydroxide. This structure-directing agent apparently precludes the formation of any MFI and is very selective for MEL. Typical molar ratios for the synthesis are as follows:

$$RN/SiO_2 = 0.10-0.25, \quad H_2O/SiO_2 = 25-50, \quad OH^-/SiO_2 = 0.20-0.30$$

$$M^+/SiO_2 = 0.05-0.15, \quad \text{temperature } 150-170\ ^\circ C$$

RN represents the templating agent and M^+ can be either Na or K cation.

Microscopy and synchrotron data: To observe the crystal morphology and fine surface structure of the as-synthesized crystal, SEM images were taken on an S-800 microscope operated at 2 kV without metal coating. ED patterns and HREM images were taken on a JEM-4000EX, objective lens with a spherical aberration coefficient of Cs = 1.0 mm, operating at 400 kV. X-ray powder diffraction data was collected at room temperature (25.5 °C) using synchrotron orbital radiation on the X7A beam line at Brookhaven National Laboratory. The all-silica MEL-type sample for X-ray diffraction was calcined to 550 °C in air and then packed into a 1 mm diameter glass capillary which was evacuated. The sample was gradually heated to 350 °C for 12 h and then sealed under vacuum. Data were collected by step scanning at 2θ intervals of 0.005° over the angular range 2−100° for a fixed time. The wavelength was determined to be 1.18551(5) Å using a Si standard.

Results and Discussion

Figure 2d shows an observed SEM image of the MEL crystals. The observed crystal morphology is consistent

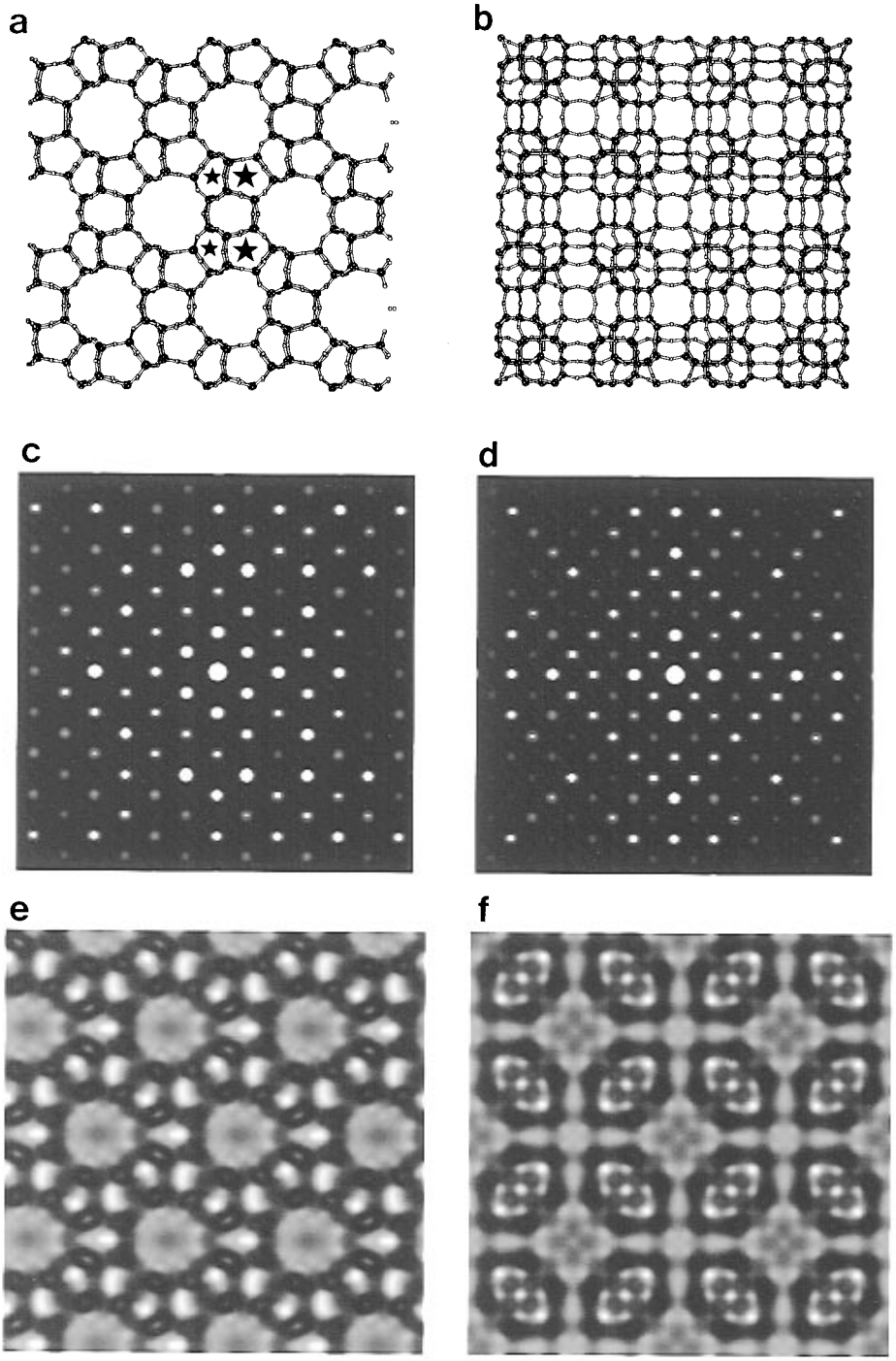

Figure 3. Projections of the framework structure of MEL-type along ⟨100⟩ ([100] or [010]) (a) and [001] (b). Simulated ED patterns (c and d) and HREM images (e and f) of MEL type along ⟨100⟩ and [001], respectively.

with the point symmetry of $\bar{4}m2$, and there is no evidence of lowering the symmetry from $\bar{4}m2$ to its subgroup of $\bar{4}$ from the micrograph.

Observed ED patterns of ⟨100⟩ and [001] are shown in Figure 4a,b, and corresponding HREM images are shown in Figure 4c,d, respectively. Both the ED pattern of Figure 4b and the HREM image of Figure 4d clearly show independently that the [001] projection of the structure has 4-fold symmetry. The HREM image of Figure 4c shows not 2-fold but rather mirror symmetry parallel to the (100) plane through the centers of both main channels and 6-rings. The fit between observed and simulated images, which is based on $I\bar{4}m2$, is very good for a series of images at different foci. All observations using EM, including the set comprised of Figure 4a,c, indicate that the crystal is pure MEL-type. We cannot observe any diffuse streaks in the ED patterns or defects in the HREM images: therefore we can conclude that a pure MEL-type crystal has been successfully synthesized by using the novel *N*,*N*-diethyl-3,5-dimethylpiperidinium hydroxide templating agent. TGA data suggested that four template molecules were accommodated per unit cell. By filling all pores with the template molecules, the formation of the MFI, i.e., intergrowth might be hindered.

We selected several crystals out of thousands for our EM study. To ensure that this conclusion applied to the whole batch, we obtained a high-resolution X-ray powder diffraction pattern, which also allowed us to determine whether this pure-silica ZSM-11 exhibited a lower symmetry than $I\bar{4}m2$ as has been suggested in earlier papers.[8−11] The crystallinity of this sample was

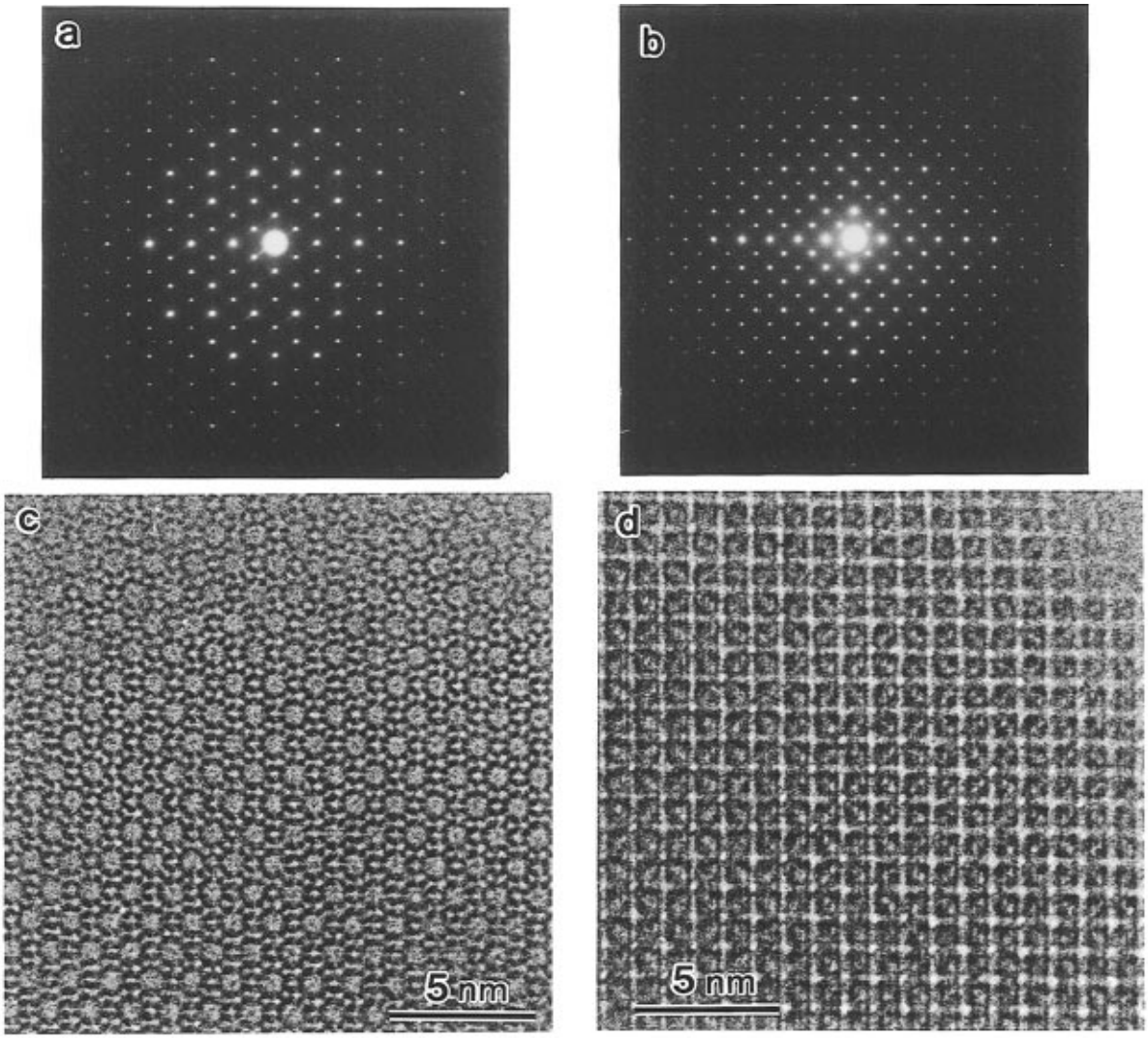

Figure 4. Observed ED patterns and HREM images of pure silica MEL type along ⟨100⟩ (a and c) and [001] (b and d), respectively.

excellent, and the intensity profiles are very sharp. It is confirmed by using DIFFaX program[13] that the intensity of 110 reflection decreases rapidly as the probability of MFI intergrowth increases and that it is still observable at a few percent of MFI intergrowth with appreciable line broadening. From the observed line width and its relative intensity, it might be said the crystal is pure MEL. This is confirmed by following Rietveld refinement with the small values of R factors. The structure refinement was carried out for the intensity data using the Rietveld technique (Rietan '94 by Dr. F. Izumi). Intensity data was well reproduced based on the previously reported tetragonal space group $I\bar{4}m2$, and it should be noted that these data were obtained at 25.5 °C. It is diffuclt to fit the profiles for small scattering angles because the profiles show asymmetry, and the atom-form factors for Si and O are very sensitive to their valence states for the small scattering vectors. Therefore the reliability factors R_{wp} and R_p increase as the minimum 2θ included for refinement decreases. The results, including the R factors, are summarized in Table 1, and the overall profile, together with the difference between observed and calculated profiles, is shown in Figure 5. To illustrate the intensity profile for small scattering angles, the profile (shown on a log scale for intensity) is inserted in the figure. Refined atomic coordinates, however, are almost the same, regardless of the angular range. Obtained bond lengths and bond angles are shown in Table 2. In

Table 1. Lattice Parameters a = 20.05988(4), b = 13.40310(3) Å[a]

atom	Wyckoff	x	y	z	B
Si(1)	8g	0.0765(4)	0.0765(4)	0.0	1.36(3)
Si(2)	16j	0.1215(3)	0.1870(3)	0.1445(5)	1.36
Si(3)	16j	0.0768(3)	0.2249(3)	0.3567(6)	1.36
Si(4)	16j	0.2792(3)	0.1888(4)	0.1395(6)	1.36
Si(5)	16j	0.3066(4)	0.0757(3)	−0.0085(4)	1.36
Si(6)	8g	0.1900(4)	0.1900(4)	0.5	1.36
Si(7)	16j	0.0756(3)	0.3800(3)	0.3564(5)	1.36
O(1)	8i	0.0894(12)	0.0	0.0266(16)	2.50(7)
O(2)	16j	0.1009(8)	0.1188(8)	0.0931(10)	2.50
O(3)	16j	0.0942(6)	0.1904(9)	0.2538(10)	2.50
O(4)	16j	0.2005(6)	0.1924(7)	0.1459(9)	2.50
O(5)	16j	0.3026(9)	0.1200(8)	0.0877(9)	2.50
O(6)	8i	0.2974(13)	0.0	0.0229(13)	2.50
O(7)	8h	0.3104(7)	0.1897(7)	0.25	2.50
O(8)	16j	0.1192(7)	0.1933(11)	0.4458(9)	2.50
O(9)	16j	0.2503(7)	0.1935(10)	0.4230(10)	2.50
O(10)	16j	0.0941(6)	0.3027(8)	0.3460(9)	2.50
O(11)	8i	0.0	0.2130(9)	0.3830(14)	2.50
O(12)	8i	0.0	0.3908(11)	0.3883(14)	2.50
O(13)	16j	0.0928(8)	0.2489(7)	0.0861(11)	2.50
O(14)	16j	0.1222(8)	0.4137(8)	0.4362(9)	2.50
O(15)	8h	0.0867(3)	0.4133(3)	0.25	2.50

[a] R_{wp} = 0.0748, R_p = 0.0584, R_e = 0.0390, R_I = 0.0470, R_F = 0.0342.

(13) Treacy, M. M. J.; Newsam, J. M.; Deem, M. W. *Proc. R. Soc. London A* **1991**, *433*, 499.

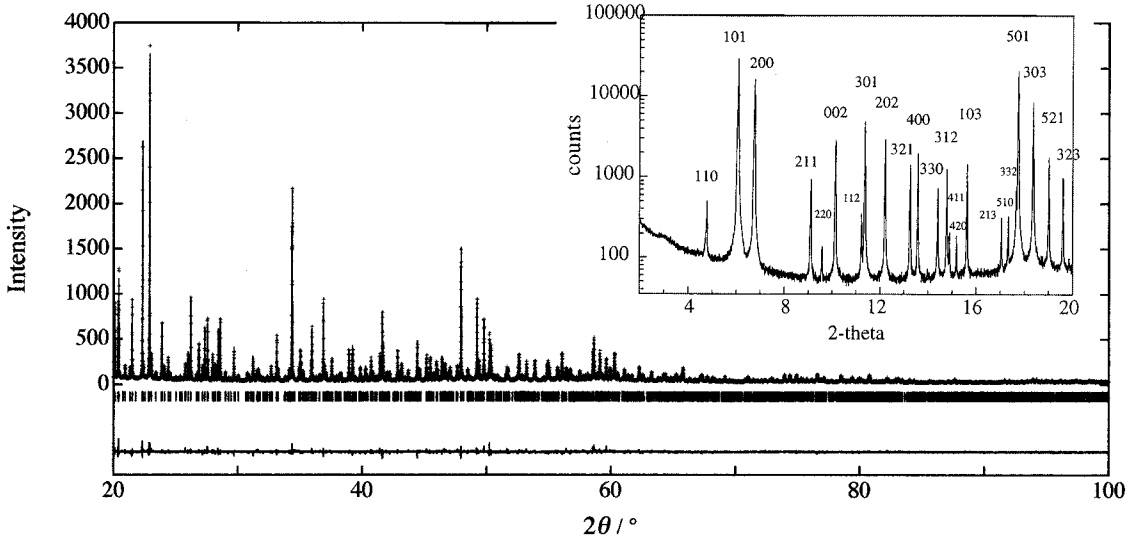

Figure 5. X-ray powder diffraction pattern of pure silica MEL type after calcination together with the difference between the observed and calculated patterns.

Table 2. Bond Lengths and Angles of All-Silica ZSM-11

bond lengths (Å)			bond lengths (Å)		
Si(1)	O(1)	1.60	Si(4)	O(7)	1.61
Si(1)	O(2)	1.59	Si(4)	O(5)	1.61
Si(2)	O(2)	1.59	Si(5)	O(5)	1.57
Si(2)	O(3)	1.56	Si(5)	O(6)	1.59
Si(2)	O(4)	1.59	Si(5)	O(13)	1.59
Si(2)	O(13)	1.58	Si(5)	O(14)	1.62
Si(3)	O(3)	1.58	Si(6)	O(9)	1.59
Si(3)	O(8)	1.60	Si(6)	O(8)	1.60
Si(3)	O(11)	1.60	Si(7)	O(14)	1.57
Si(3)	O(10)	1.61	Si(7)	O(15)	1.59
Si(4)	O(9)	1.58	Si(7)	O(12)	1.59
Si(4)	O(4)	1.58	Si(7)	O(10)	1.60

bond angles (deg)		bond angles (deg)	
Si(1)−O(1)−Si(1)	148.1	Si(4)−O(9)−Si(6)	161.4
Si(2)−O(2)−Si(1)	152.0	Si(7)−O(10)−Si(3)	152.2
Si(2)−O(3)−Si(3)	155.8	Si(3)−O(11)−Si(3)	149.2
Si(4)−O(4)−Si(2)	172.4	Si(7)−O(12)−Si(7)	144.9
Si(5)−O(5)−Si(4)	148.5	Si(5)−O(13)−Si(2)	167.1
Si(5)−O(6)−Si(5)	146.4	Si(7)−O(14)−Si(5)	152.9
Si(4)−O(7)−Si(4)	149.0	Si(7)−O(15)−Si(7)	157.3
Si(6)−O(8)−Si(3)	146.2		

addition to these small R factors, the refined values based on the space group $I\bar{4}m2$ take a narrow range between 1.56 and 1.62 Å for the Si−O bond length and reasonable values between 145 and 172° for the Si−O−Si angle. This is in contrast to the previous report by Fyfe et al. which reports a wide range of Si−O bond lengths, in particular, a short length of 1.49 Å and long length of 1.68 Å.[5] We also tried to fit the observed intensity profile based on an $I\bar{4}$ space group using the same refinement procedure. The atomic coordinates obtained were almost the same as those obtained using the higher symmetry of $I\bar{4}m2$, as were the R factors. It is diffult to determine which space group should be chosen, but we have observed a temperature dependence of lattice constants which may suggest that the transformation occurs just above room temperature.[14] These findings suggest that it will be necessary to perform similar temperature-dependent ^{29}Si MAS NMR experiments on the present specimen in order to determine whether it undergoes similar phase transformations as has been previously reported.[4−7]

Acknowledgment. We would like to acknowledge the assistance of Dr. G. Zhang from Chevron Research and Technology Co. in collecting the synchrotron data (XRD data collected at X7A beam line, National Synchrotron Light Source, Brookhaven National Laboratory, which is supported by the U.S. Department of Energy, Division of Materials Sciences and Division of Chemical Sciences), and G. Mondo and K. Ong for preparing the sample for the synchrotron experiment. We also acknowledge the preliminary Rietveld refinement work of Dr. T. V. Harris of Chevron Research and Technology Co. O.T. thanks financial support from Minstry of Education, Science and Culture, Japan. Sumitomo Chemical Co., Nippon Sheet Glass Foundation for Material Science and Technology Foundation are also acknowledged for partial support. Y.N. wishes to thank Dr. S. I. Zones for helpful discussions, G. S. Lee for assistance in ZSM-11 syntheses, Dr. I. Y. Chan for preliminary electron diffraction studies on the MEL samples, and Chevron Research and Technology Co. for permission to publish this work.

CM950387I

(14) Sakuma, H.; Terasaki, O.; Nakagawa, Y., to be submitted.